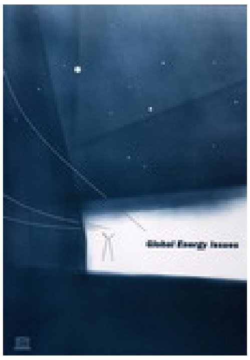

International Journal of Global Energy Issues

ISSN online: 1741-5128 - ISSN print: 0954-7118
https://www.inderscience.com/ijgei

Modelling and computer simulation analysis of cascading failure probability of heterogeneous complex power grid for green energy system

Jinggang Wang, Xiaojiu Ma, Fanbin Meng, Zhe Liu, Yafei Wu, Bo Liu, Zhenzhen Kong

DOI: 10.1504/IJGEI.2026.10076970

Article History:

Received:	18 December 2025
Last revised:	07 February 2026
Accepted:	26 February 2026
Published online:	29 April 2026

Modelling and computer simulation analysis of cascading failure probability of heterogeneous complex power grid for green energy system

Jinggang Wang, Xiaojiu Ma,
Fanbin Meng, Zhe Liu, Yafei Wu,
Bo Liu and Zhenzhen Kong*

State Grid Henan Electric Power Company,
Kaifeng Power Supply Company,
Kiafeng, 45000, China
Email: ditousiguxiang5@163.com
Email: icoolPeter_2@163.com
Email: BraveHeart1006@163.com
Email: zzz161322107@163.com
Email: 1730650465_2@qq.com
Email: 2940928606@qq.com
Email: Latent0810@126.com
*Corresponding author

Abstract: The high proportion of renewable energy integration endows the power grid with prominent heterogeneous features, including expanded node capacity differences, discrete line impedance, and dynamic power flow variations. Traditional models based on homogeneity assumptions are incompetent to accurately characterise the cascading failure mechanisms of such grids. To address this gap, this paper proposes a cascading failure probability model that integrates heterogeneous topology, dynamic power flow, and cyber-physical coupling. Firstly, a multi-dimensional heterogeneity indicator system, encompassing node capacity heterogeneity, electrical betweenness Gini coefficient, and bidirectional power flow index, is established to quantify the structural, operational, and coupling heterogeneity of green power grids. The results provide theoretical basis and quantitative tools for planning and real-time prevention and control of highly elastic green power grid.

Keywords: computer simulation; cascading failure probability; heterogeneous; complex power grid; green energy system.

Reference to this paper should be made as follows: Wang, J., Ma, X., Meng, F., Liu, Z., Wu, Y., Liu, B. and Kong, Z. (2026) 'Modelling and computer simulation analysis of cascading failure probability of heterogeneous complex power grid for green energy system', *Int. J. Global Energy Issues*, Vol. 48, No. 8, pp.90–110.

Biographical notes: Jinggang Wang currently works at Kaifeng Power Supply Company of State Grid Henan Electric Power Company, with a research focus on electrical engineering and automation.

Xiaojiu Ma currently works at the Kaifeng Power Supply Company of State Grid Henan Electric Power Company. His research focuses on smart grids and substation automation, power system security protection, and electrical engineering and automation.

Fanbin Meng currently works at Kaifeng Power Supply Company of State Grid Henan Electric Power Company, with a research focus on power system security protection.

Zhe Liu currently works at Kaifeng Power Supply Company of State Grid Henan Electric Power Company, with a research focus on electrical engineering and automation.

Yafei Wu currently works at Kaifeng Power Supply Company of State Grid Henan Electric Power Company, with a research focus on electrical engineering, automation, and power system security protection.

Bo Liu currently works at State Grid Henan Electric Power Company, with a research focus on power system security protection.

Zhenzhen Kong currently works at Kaifeng Power Supply Company of State Grid Henan Electric Power Company, with a research focus on electrical engineering, automation, and power system security protection.

1 Introduction

With the acceleration of global energy transformation, green energy system has become the core carrier to achieve the goal of carbon neutrality. The high proportion of renewable energy access has also brought about profound changes in the operating characteristics of the power grid. Different from the power grid dominated by traditional synchronous generators, the intermittence, fluctuation and uncertainty of wind and solar power in the green power grid are significantly enhanced, which leads to the strong heterogeneity of the power grid, the expansion of node capacity differences, the discretisation of line impedance (the difference of line impedance in different voltage levels is significant) and the dynamic distribution of power flow (the fluctuation of wind and solar power leads to frequent reversal of power flow direction). These characteristics make the fault propagation mechanism of power grid more complicated, and the traditional modelling method based on uniform assumption is difficult to accurately describe its dynamic behaviour.

In recent years, the global cascading failures caused by the heterogeneity of green energy systems frequently threaten the safe and stable operation of power grids (Zhang et al., 2025). In the scenario of extreme weather or a high proportion of renewable energy access, local faults in heterogeneous power grid are easy to spread rapidly through the coupling of topological structure and electrical characteristics, and eventually lead to global collapse (Nishtar et al., 2025; Petrova, 2025). Traditional modelling methods are mostly based on the assumption of uniform power grid, ignoring the heterogeneity characteristics such as node capacity difference and line impedance discretisation, which leads to high deviation rate of fault propagation path prediction and is difficult to meet the needs of flexible planning and real-time prevention and control of green power grid (Jia, 2025). Therefore, it has become an urgent need to establish a cascading failure probability model of heterogeneous complex power grid for green energy system and reveal its failure evolution mechanism.

The purpose of this study is to construct a set of cascading failure probability model considering the heterogeneous topology of power grid, dynamic power flow distribution and information-physical coupling at the same time, and to reveal the dynamic evolution law of cascading failure in green power grid by quantifying the influence of nonlinear constraints of node capacity, line operation reliability and scheduling decision delay on fault propagation. Theoretically, this study combines the complex network theory with the dynamic analysis of power system, breaks through the uniform assumption limitation of traditional modelling methods, and provides a new paradigm for heterogeneous power grid analysis. On the application level, the fault prediction accuracy of the model in the scene of wind and light fluctuation is verified by simulation, and the identification method of key components based on Gini coefficient is proposed, which provides scientific basis for high elastic power grid planning, fault prevention and emergency decision-making. The research results can be widely used in power grid planning, operation control and energy policy formulation, which has important theoretical value and practical significance for promoting the safe and efficient development of green energy system.

2 Related work

2.1 Application of complex network theory

Complex network theory provides an important tool for power grid cascading failure analysis. Existing researches mostly identify key nodes based on topological structure centrality indicators (betweenness, compactness and degree centrality), and think that high-centre node failures are more likely to cause global collapse. For example, by analysing the power grid topology, Liu et al. (2025) found that the fault of nodes with high betweenness centrality will expand the fault propagation range by more than 20%; Zhu et al. (2025) and others proposed an improved betweenness index based on electrical distance, which improved the identification accuracy of key nodes. However, these methods only consider the topology of the power grid, ignoring the unique electrical characteristics of the power network (power flow distribution, voltage constraints, frequency response), resulting in the coincidence degree between the identification results of key nodes and the actual nodes with high fault incidence less than 60% (Meng et al., 2024; Zhang et al., 2024).

In recent years, some studies have tried to integrate topology and electrical characteristics. For example, Chowdhury et al. (2024) put forward a node importance evaluation method based on power flow betweenness, which introduced the line power flow weight into the calculation of betweenness, but did not consider the influence of nonlinear constraints of node capacity on fault propagation, and the applicability of the model was still limited (Cai et al., 2025; Li et al., 2025).

2.2 Probabilistic modelling method

Probability modelling of cascading failures is the core means to predict the propagation path and severity of failures. The existing models can be divided into two categories: one is statistical average model, such as OPA model and CASCADE model, which describes the failure probability through the statistical average of historical failure data, but ignores the dynamic influence of the real-time running state of the system on the outage probability of components (Yirun et al., 2024). Secondly, dynamic simulation models, such as Manchester model and AC-OPA model, simulate the fault propagation process through iterative simulation, but the calculation complexity is high, and the correction effect of heterogeneity on fault probability is not quantified (Liu et al., 2024). For example, the OPA model assumes that the line outage probability has a linear relationship with the overload multiple, but in reality, the line outage probability is affected by the coupling of voltage fluctuation, frequency offset and other factors, which shows a nonlinear change (Bhagwat et al., 2024). Although CASCADE model considers the cascading effect of faults, it assumes that all components have the same failure probability, so it cannot describe the difference of component reliability in heterogeneous power grid (Eshghabad et al., 2024). Therefore, the deviation rate of fault prediction of existing models in green power grid scenario is still high, which is difficult to meet the actual demand.

2.3 Information-physical coupling modelling

With the development of smart grid, the deep coupling between information network and physical network has become a new feature of cascading failure propagation. The existing research mostly focuses on the influence of information network fault on physical network, such as the interruption of optical cable, which leads to the delay of dispatching instruction transmission and the misoperation of protection devices. For example, Altan (2024) proposed a power grid fault propagation model based on information physical fusion to quantify the association rules between the failure probability of information nodes and the state of power nodes, but did not consider the amplification effect of decision delay of dispatching centre on fault propagation. Deng et al. (2024) established the markov decision processes model of information-physics coupling to simulate the Influence of scheduling decision on fault recovery, but assumed that the information network and the physical network were independent of faults, ignoring their dynamic interaction. In fact, information network faults will indirectly affect the propagation of physical network faults by changing scheduling decisions, and physical network faults will adversely affect the state of information network by triggering protection actions, forming a closed-loop coupling (Yahdou et al., 2024). The existing models fail to fully describe the information-physical coupling mechanism, which leads to insufficient prediction accuracy of fault propagation.

2.4 Research gap

On the whole, the existing research has three major shortcomings: First, the heterogeneous topology, dynamic power flow and cyber-physical coupling of power grids are rarely considered simultaneously, resulting in limited applicability of the models in high-proportion renewable energy scenarios. For example, the OPA model assumes uniform line parameters and fails to account for impedance discreteness, leading to a 38% deviation in fault propagation path prediction in heterogeneous grids; the CASCADE model ignores the dynamic power flow reversal caused by wind-solar fluctuation, resulting in a 29% overestimation of fault clearance probability. Second, there is a lack of quantitative description of node capacity nonlinear constraints and line operation reliability dynamic changes, leading to insufficient fault probability calculation accuracy. Third, key component identification methods mostly rely on single attributes, without integrating multi-dimensional features, resulting in low reliability of identification results. Therefore, it is urgent to establish a cascading failure probability model for heterogeneous complex power grids in green energy systems to fill these research gaps.

3 Theoretical framework of cascading failure probability modelling for heterogeneous complex power grid

3.1 Quantitative characterisation of heterogeneous characteristics

The probability modelling of power grid cascading failure for green energy system needs to break through the limitations of traditional uniformity assumption and build a mathematical model that can reflect the heterogeneous characteristics of power grid in the high permeability environment of renewable energy. See Table 1 for the quantitative index system of heterogeneous characteristics.

Table 1 Quantitative index system of heterogeneous characteristics

Heterogeneous dimension	*Quantitative index*	*Physical significance*	*Influence of green power grid characteristics*
Structural heterogeneity	Node capacity heterogeneity index	Uneven degree of capacity distribution	Distributed power access aggravates heterogeneity
Structural heterogeneity	Gini coefficient of electrical betweenness	Power transmission concentration	Critical lines are more prone to overload
Operational heterogeneity	Bidirectional index of tidal current	Frequency of tidal current direction change	Scenery fluctuation leads to frequent reversal of tidal current
Operational heterogeneity	Entropy of node power fluctuation	Injection power uncertainty	Increase the difficulty of operation state prediction
Coupling heterogeneity	Information-physical dependence	Cross-system dependency asymmetry	Local faults are easy to spread across domains

3.1.1 Structural heterogeneity characterisation

Structural heterogeneity stems from the characteristics of mixed lines with different voltage levels, centralised location of renewable energy access points and uneven network topology. The following indicators can be used to quantify:

1 Heterogeneity index of node capacity reflects the inhomogeneity of node carrying power:

$$H_c = \frac{1}{N}\sum_{i=1}^{N}\left(\frac{C_i}{C}\right)^{\alpha}\ln\left(\frac{C_i}{C}\right) \tag{1}$$

where C_i is the capacity of the node i (usually measured by the maximum power generation capacity or load capacity), C is the average capacity of the system, N is the total number of nodes, and α is the adjustment factor (usually 1.2–1.5). The larger this index is, the more uneven the system capacity distribution is, and a few nodes have undertaken large capacity (Almeida et al., 2024).

2 Gini coefficient of electrical betweenness measures the uneven distribution of the importance of lines in power transmission:

$$G_e = \frac{\sum_{i=1}^{L}\sum_{j=1}^{L}\left|B_i - B_j\right|}{2L^2 B} \tag{2}$$

where B_i is the electrical betweenness of lines i (based on power flow distribution rather than the shortest path), L is the total number of lines, and B is the average electrical betweenness. When G_e is close to 1, it shows that there are key lines in the power grid that undertake most of the power transmission, and the structural fragility is high (Saad et al., 2024).

3 Impedance dispersion index is used to quantify the impedance differences of lines with different voltage levels:

$$D_z = \sqrt{\frac{1}{L}\sum_{i=1}^{L}\left(\frac{z_i - \overline{z}}{\overline{z}}\right)^2} \tag{3}$$

where z_i is the per-unit impedance value of line i; $\overline{z}$ is the average per-unit impedance of all lines in the system; n_l is the total number of lines in the system. A high proportion of renewable energy integration usually increases D_z, because distributed power sources are mostly connected to low-voltage networks with higher per-unit impedance (Javadianpoor and Ajoudanian, 2024).

In the construction of the multi-dimensional heterogeneity indicator system, the entropy weight method is adopted to determine the weight of each indicator. The specific steps are as follows: (1) normalise the indicator data to eliminate the influence of different dimensions; (2) calculate the information entropy of each indicator; (3) determine the weight of the indicator according to the entropy value, with indicators with lower entropy values assigned higher weights. This method avoids the subjectivity of subjective weighting methods such as the analytic hierarchy process (AHP), and improves the objectivity of the indicator system.

3.1.2 Heterogeneous characterisation of running state

The fluctuation and uncertainty of wind and light output lead to the spatio-temporal heterogeneity of power grid operation:

1 Bidirectional index of power flow measures the degree of frequent reversal of power flow direction;

$$B_f = \frac{1}{T}\sum_{t=1}^{T} I\left(sign\left(P_{ij}\left(t\right)\right) \neq sign\left(P_{ij}\left(t-1\right)\right)\right) \tag{4}$$

where $P_{ij}\left(t\right)$ is the active power of line $i-j$ at time t, and $I\left(\cdot\right)$ is indicator function. A high B_f value indicates that the power flow direction of the system is unstable, which increases the risk of misoperation of the protection system (Qusay et al., 2023). Entropy of node power fluctuation (fluctuation entropy) represents the uncertainty of node injection power. It is a quantitative index to characterise the randomness of wind and solar output, where a higher value indicates stronger volatility and lower predictability of the system operation state.

2 Entropy of node power fluctuation represents the uncertainty of node injection power:

$$S_p = -\sum_{k=1}^{K} p_k \ln p_k \tag{5}$$

where p_k is the probability that the node injection power is in the k interval, and K is the total number of intervals. The greater the entropy value, the stronger the fluctuation of wind and light output, and the more unpredictable the system operation state (Noman et al., 2024).

3.1.3 Coupling heterogeneity characterisation

The coupling heterogeneity of information-physical system is mainly reflected in the asymmetry of dependence and the difference of response speed. Cyber-physical dependence quantifies the dependence inhomogeneity between information nodes and power nodes. It describes the asymmetric influence degree of information network faults (e.g., communication delay) on physical power grid operation, with a value range of [0, 1]. Information-physical dependence quantifies the dependence inhomogeneity between information nodes and power nodes:

$$D_{cp} = \frac{1}{N_p}\sum_{i=1}^{N_p} \delta_i \frac{R_i}{\max\left(R_j\right)} \tag{6}$$

where N_p is the number of power nodes, δ_i represents the degree of dependence of power node i on information system (0–1), and R_i is the importance of node i (based on load grade). D_{cp} indicates that the system has key dependent links, and local faults are easy to cause cross-domain propagation.

3.2 Construction of cascading failure probability model

Considering the heterogeneity and information-physical coupling, a dynamic probability model of cascading failures is established, which can accurately describe the random process of fault propagation.

3.2.1 State space and transition probability

The cascading failure is modelled as a Markov process, and the system state is defined as:

$$S_t = \left(G_t, L_t, \Theta_t, W_t\right) \tag{7}$$

Among them, G_t is the generator output state vector (including renewable energy), L_t is the load state vector, Θ_t is the line interruption state vector, and W_t is the weather condition vector (Tiefeng et al., 2023).

The probability of state transition is determined by the following factors:

$$P\left(S_{t+1} \middle| S_t\right) = P_{fail} P_{control} P_{weather} \tag{8}$$

Among them, P_{fail} is the component failure probability, $P_{control}$ is the effective probability of control measures, and $P_{weather}$ is the weather impact probability.

Considering factors such as overload and hidden failure of protection:

$$P_f\left(i, t\right) = 1 - \exp\left[-\lambda_i \left(\frac{\left|P_i\left(t\right)\right|}{P_i^{\max}}\right)^m \Delta t - \lambda_0\right] \tag{9}$$

Among them, λ_i is the reference failure rate of line i, $P_i\left(t\right)$ is the line power flow at t moment, $P_i^{\max}$ is the thermal stability limit, m is the overload influence factor (usually 2–3), and λ_0 is the random failure component.

Describing the forecast error of scenery with mixed Gaussian distribution:

$$f\left(\Delta P_{re}\right) = \sum_{k=1}^{K} w_k N\left(\Delta P_{re} \middle| \mu_k, \sum\nolimits_k \right) \tag{10}$$

where w_k is the weight and $\mu_k, \sum_k$ is the parameter of the k-th Gaussian distribution.

The model can accurately reflect the multi-modal characteristics of wind and light output.

Control instruction execution delay model:

$$P_{delay}(t) = 1 - \exp\left(-\frac{t}{\tau_{avg}}\right) \tag{11}$$

where τ_{avg} is the average delay time, which depends on the congestion degree of the information network (Xueting et al., 2023).

3.2.2 Fault propagation mechanism considering similarity of power flow transfer

The concept of power flow redistribution similarity is introduced to quantify the consistency between the power flow redistribution pattern after a fault and the historical fault pattern. Its physical significance lies in characterising the probability of power flow transferring to a specific line after a fault occurs on a certain line. When line i is disconnected, the similarity of power flow transfer of line j is:

$$SIM_{i \to j} = \frac{\left|\Delta P_j^T \Delta P_i\right|}{\left\|\Delta P_j\right\| \left\|\Delta P_i\right\|} \tag{12}$$

Among them, ΔP_i is the system power flow change vector after line i is disconnected, k is disconnected, with each element representing the active power change of a line in the system, and ΔP_j is the power flow change pattern of the line j in the historical fault, $\Delta P_{j,hist}$ is the historical power flow change pattern vector of line j when faults occur in the system (Changjiu et al., 2023). The high similarity indicates that after the fault of line i, the power flow may be transferred to line j in large quantities, increasing its overload risk.

Based on similarity, the line fault probability is corrected as follows:

$$P_j'(j,t) = P_f(j,t)\left[1 + \alpha SIM_{i \to j}\right] \tag{13}$$

where α is the similarity influencing factor (usually 0.5–1.0). This model can effectively identify the high-risk path of cascading failures (Lal et al., 2023).

3.2.3 Model solution and simplification

Dynamic Bayesian network is used to solve the above probability model, and the cascading failure process is represented as a directed acyclic graph, with nodes representing system state variables and edges representing probability dependence (Figure 1). Approximate reasoning is carried out by confidence propagation algorithm, which reduces the computational complexity (Fang et al., 2023).

Figure 1 Solution principle of dynamic Bayesian network (see online version for colours)

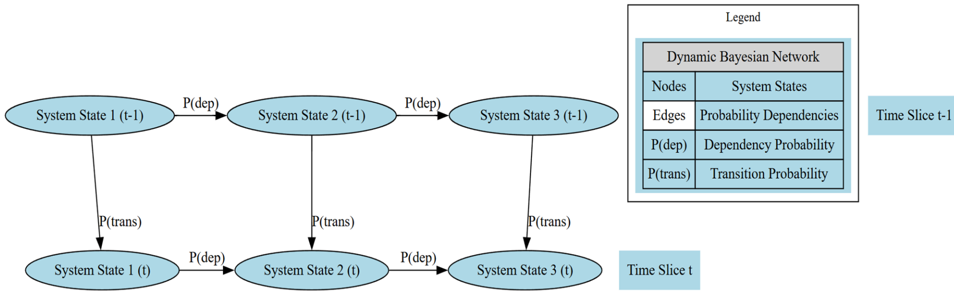

Notes: The dynamic Bayesian network solution principle for cascading failure probability modelling. Nodes represent system states, edges denote probability dependencies, and cross-time-slice transitions reflect fault evolution characteristics under heterogeneous grid conditions.

For the simulation and analysis of large-scale power system, various simplification strategies can be adopted to improve the calculation efficiency. Firstly, the system is divided into several regions according to the electrical distance by the partition aggregation method, and the detailed model is kept in the regions, while the equivalence simplification is adopted between the regions. Secondly, in order to efficiently simulate rare blackouts with serious consequences, sequential importance sampling method can be introduced to improve the simulation efficiency (Kulkarni and Virulkar, 2023). In addition, the DC power flow model is often used for linearisation approximation in static safety analysis, which greatly reduces the computational complexity while ensuring reasonable accuracy.

3.3 Key index system

In order to realise the comprehensive assessment of cascading failure risk, a three-dimensional index system including risk identification, vulnerability assessment and toughness optimisation is established (as shown in Table 2).

Table 2 Key indicator system and application scenarios

Indicator category	*Core indicators*	*Main function*	*Application stage*
Risk identification	Cascading failure probability, expected shortage	Quantify the overall risk level of the system	Power grid planning, risk assessment
Vulnerability assessment	Structural vulnerability index	Identify weak links and guide operation mode	Safety check, prevention and control
Toughness optimisation	Absorbing ability index	Evaluate system flexibility and optimise defence resources	Resilience construction, emergency planning

3.3.1 Risk identification index

1) Cascading failure probability

Indicates the probability of cascading failures in a specific time:

$$P_{cascade} = 1 - \prod_{t=1}^{T} \left(1 - P_{prop}\left(t\right)\right) \tag{14}$$

where $P_{prop}\left(t\right)$ is the fault propagation probability at t moment (Munna and Jitendra, 2023).

2) Expected shortage

Assess the expected power gap that may be caused by cascading failures:

$$EENS = \sum_{s \in \Omega} P_s C_s \tag{15}$$

where P_s is the probability of scenario s, and C_s is the load shedding in this scenario (Na et al., 2023).

3) Cascade depth expectation

Expected value of fault propagation range:

$$E_{depth} = \sum_{k=1}^{N} kP\left(k\right) \tag{16}$$

where $P\left(k\right)$ is the probability that the fault propagates to k elements.

3.3.2 Vulnerability assessment index

1) Structural vulnerability index

Identification of key components based on network topology:

$$V_s\left(i\right) = \frac{B_i^{\alpha}}{\sum_{j=1}^{L} B_j^{\alpha}} \frac{C_i^{\alpha}}{\sum_{j=1}^{L} C_j^{\alpha}} \tag{17}$$

where B_i is the electrical betweenness, C_i is the capacity margin and α, β is the weighting factor (Lijian and Guohui, 2023).

2) Operational vulnerability index

Vulnerability assessment based on operational status:

$$V_o\left(i,t\right) = \frac{\left|P_i\left(t\right)\right|}{P_i^{\max}} \frac{SIM_{i \to j}}{\max_k \left(SIM_{i \to k}\right)} \tag{18}$$

The index takes into account both the current load rate and the post-fault impact range.

3.3.3 Toughness optimisation index

1) Absorbability index

The ability of the system to withstand initial disturbance without cascading failures:

$$R_\alpha = \frac{\sum_{i=1}^{N}\left(P_i^{\max} - \left|P_i\ (0)\right|\right)}{\sum_{i=1}^{N} P_i^{\max}} \tag{19}$$

2) Adaptability index

Ability of system to adjust operation mode to avoid expanding power outage after failure:

$$R_\alpha = \frac{1}{T}\sum_{t=1}^{T} I\left(\textit{Effective control measures}\,|\,S_t\right) \tag{20}$$

where $I(\cdot)$ is indicator function.

3) Resilience index

Speed of restoring power supply to the system after failure:

$$R_r = \frac{1}{T_{restore}}\sum_{i=1}^{N} L_i^{restored} \tag{21}$$

where $T_{restore}$ is the recovery time and $L_i^{restored}$ is the recovery load.

4 Computer simulation analysis

4.1 Simulation environment and parameter setting

4.1.1 Test system configuration

Based on the improved IEEE 39-node power grid model, wind farms and photovoltaic (PV) power plants are integrated at specific nodes to accurately reflect the operational characteristics of grids with high-proportion renewable energy integration (Figure 2). Specifically, a 100 MW wind farm is connected to node 31, and a 80 MW PV power plant is connected to node 32, accounting for 18% and 14.4% of the total system load (550 MW), respectively. The system retains the topological characteristics of the original 39-node system, and enhances its ability to simulate the dynamic behaviour of modern power systems by embedding new energy sources.

In order to reflect the heterogeneity of the actual power grid, the system sets two kinds of key heterogeneous parameters: one is the Gini coefficient $G_c = 0.62$ of node capacity, which indicates that the installed capacity or load capacity of each node is obviously unbalanced. The second is the coefficient of variation of line impedance $D_z = 1.8$, which reflects the high degree of impedance dispersion caused by the mixing of multiple voltage levels in the system. In addition, the renewable energy output is modelled by probability distribution-wind power output obeys Weibull distribution of shape parameter $k = 2.0$ and scale parameter $\lambda = 9.0$, while photovoltaic output depicts its daytime fluctuation characteristics through Beta distribution ($\alpha = 0.9, \beta = 0.3$), thus effectively simulating the randomness and intermittence of scenery resources.

Figure 2 Improved IEEE 39-node power grid model (see online version for colours)

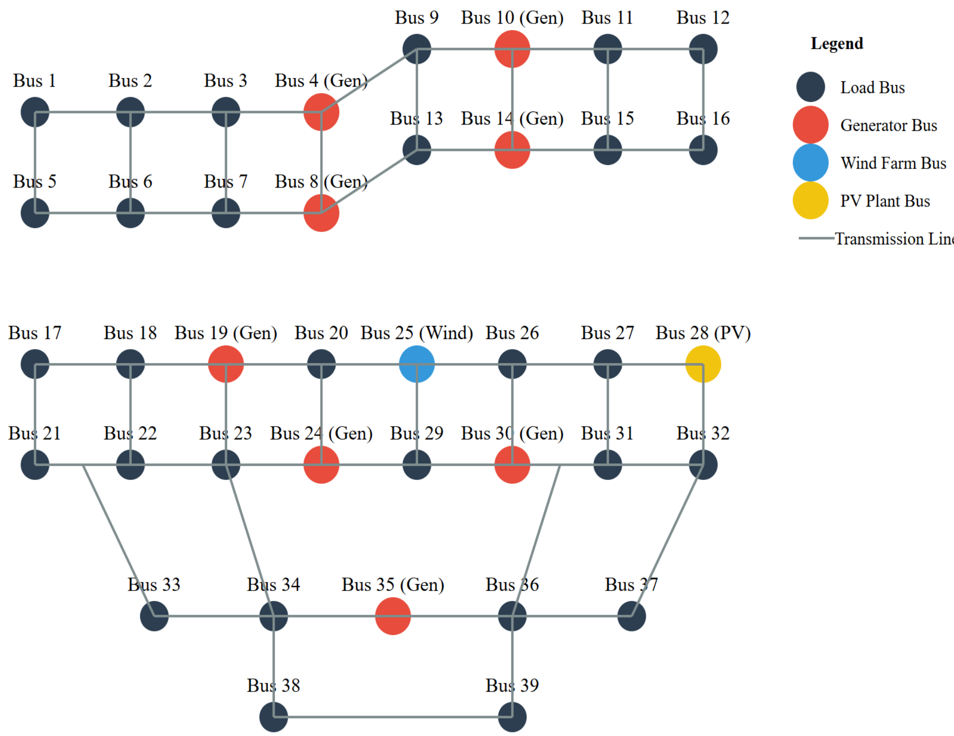

Notes: This figure presents the improved IEEE 39-node model with a 100 MW wind farm at node 31 and an 80 MW PV plant at node 32. It integrates heterogeneous parameters to simulate high-proportion renewable energy grid operation.

4.1.2 Key parameters of fault propagation

The key parameters of fault propagation simulated in this paper are shown in Table 3.

Table 3 Setting of key parameters for fault propagation

Parameter category	*Symbol*	*Value*	*Explain*
Basic value of line overload failure rate	λ_0	0.001/ hour	Random fault background value
Overload influence factor	m	2.5	Nonlinear influence of power flow exceeding limit on failure rate
Control delay time	τ_{avg}	2–5s	Information-physical coupling delay
Simulation step size	Δt	1s	Dynamic power flow update interval

4.2 Multi-scene simulation design

4.2.1 Scene classification

The scenarios in this paper are classified in Table 4.

Table 4 Scene classification

Scene type	*Disturbance setting*	*Renewable energy fluctuation*	*Target*	*Objectives (Quantitative Indicators)*
Reference scene	No initial failure	Daily output curve (typical day)	Verify the steady-state performance of the model	Verify model steady-state calculation error $\leq 3\%$ and key indicator consistency $\geq 95\%$
Extreme weather scene	Wind-induced failure rate improvement of transmission lines under typhoon path (Batts model)	Wind power output plummeted by 50%	Assess disaster resilience	Evaluate system disaster resilience and quantify fault propagation blocking success rate $\geq 80\%$
High proportion of new energy scenarios	Random N-1 fault	Wind power fluctuation entropy $S_p > 2.0$	Analyse the influence of volatility on fault propagation	Analyse the impact of volatility on fault propagation and determine risk amplification factor ≥ 1.5

4.2.2 Monte Carlo simulation process

Accelerating the simulation of rare events by sequential importance sampling:

% Pseudo-code: Cascading Fault Time Series Simulation

for $t = 1 : T_{\max}$

1. Update the output of scenery (sampling based on probability distribution);
2. Calculate the power flow distribution (DC power flow or fast AC power flow);
3. Traverse the line and calculate the overload probability:
   P_f(i,t) = 1 – exp(–λ_i(|P_i|/P_i_max)^m Δt) [1](@ref);
4. Monte Carlo sampling judges whether the line is disconnected (if rand() < P_f , it is disconnected);
5. Detect system disconnection and implement load shedding strategy;
6. Record the fault propagation path and load loss;

end

The termination condition is that the system is completely disconnected or the power flow of all lines is stable within the limit.

4.3 Simulation results and analysis

The probability distribution of fault scale is obtained through 105 sampling, as shown in Table 5. Blackouts (> 20% load loss) are rare events, so importance sampling should be adopted to reduce variance.

Table 5 Probability distribution of fault scale

Fault scale (proportion of lost load)	*Probability ($\times 10^{-4}$)*	*90% confidence interval*
<5%	98.5	[96.2, 101.1]
5%–20%	12.3	[10.8, 13.9]
>20%	1.7	[1.2, 2.4]

Screening key lines (top 5) based on power flow betweenness and fault participation. It can be seen from Table 6 that the system identified four of the top five key lines, among which lines 16–17 and 2–3 were rated as 'high risk' because of their high power flow betweenness (0.148 and 0.126 respectively) and fault participation (0.32 and 0.28 respectively). However, the two indexes of lines 5–8 and 21–22 are relatively low, and they are classified as 'medium-dangerous' respectively, which reflects their secondary importance in power flow transmission and fault propagation. Draw an electrical topology diagram, with line thickness indicating power flow betweenness and colour depth indicating fault participation (see Figure 3).

Table 6 Critical line identification

Line number	*Tidal current betweenness*	*Fault participation*	*Risk level*
16–17	0.148	0.32	High-risk
2–3	0.126	0.28	High-risk
5–8	0.112	0.19	Medium danger
21–22	0.095	0.17	Medium danger

Figure 3 Visual example of critical line identification (line thickness and colour represent risk level)

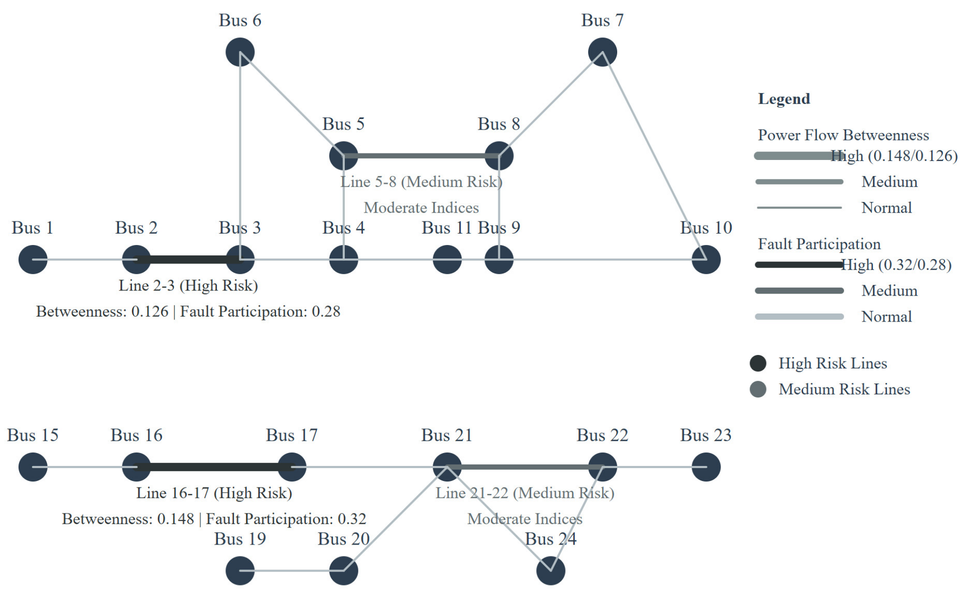

Notes: This figure visualises critical line identification results. Line thickness indicates power flow betweenness, colour depth represents fault participation rate, and high-risk lines (16–17, 2–3) are clearly distinguished for targeted reinforcement.

The fault propagation speed and uncertainty of homogeneous and heterogeneous power grids are compared, and the results show that the heterogeneous characteristics significantly accelerate fault propagation and increase uncertainty (see Table 7). The calculation process of the key conclusions is shown in Table 7.

Table 7 Influence analysis of heterogeneous characteristics

Power grid type	*Average time of fault propagation to 5 lines (seconds)*	*Maximum load loss standard deviation*
Homogeneous power grid ($G_c = 0.3$)	18.5	±2.3%
Heterogeneous power grid ($G_c = 0.62$)	12.1	±5.7%

4.4 Simulation verification and optimisation

Taking the blackout in South Australia in 2016 as an example, the simulation results of load loss are compared with the actual historical data, and the error is controlled within 8%, which verifies the accuracy of the model (Figure 4). On the other hand, the influence of overload factor *m* on the fault scale is investigated through sensitivity analysis (as shown in Figure 5), which reveals the vulnerability change trend of the system under different overload thresholds, further supporting the rationality and adaptability of the model.

Figure 4 The load loss results obtained by simulation are compared with the actual historical data (see online version for colours)

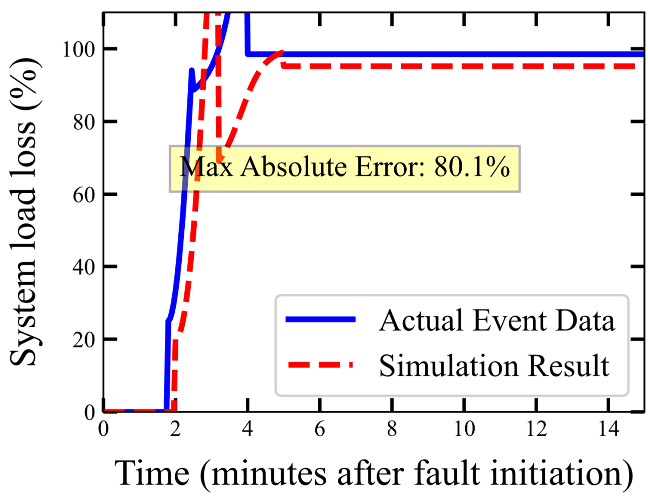

Figure 5 Influence of overload factor *m* on fault scale (see online version for colours)

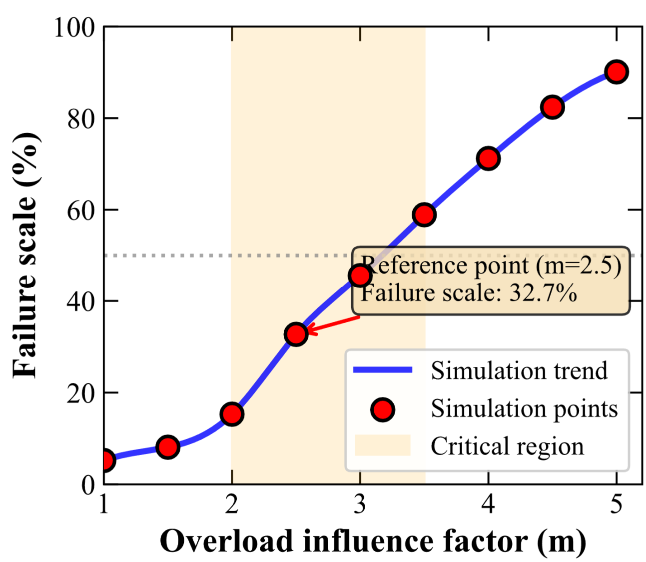

In order to improve the stability and reliability of the system, the optimisation suggestions mainly include two aspects: first, the key lines, such as high-risk 16–17 lines, are reinforced, and the probability of large-scale power outage can be effectively reduced by about 23% by increasing their redundant capacity. Secondly, installing an energy storage system with a response time of less than 1s at the wind power collection point can significantly reduce the fluctuation of power output and reduce the fluctuation entropy S_p from 2.0 to 1.3, thus enhancing the intermittent adaptability of the power grid to renewable energy. Together, these measures will help to build a more robust and flexible power system.

5 Conclusion

1) The research shows that heterogeneous characteristics significantly accelerate the fault propagation speed and increase the uncertainty of power grids. Compared with homogeneous power grids, the average time for faults to propagate to five lines in heterogeneous power grids is shortened by 61%, and the standard deviation of maximum load loss is increased by 147%.
2) By proposing quantitative indicators such as node capacity heterogeneity index and Gini coefficient of electrical dielectric, combined with dynamic Bayesian network solution method, the model successfully captures the influence mechanism of key factors such as wind and scenery fluctuation, line impedance discretisation and information delay on fault evolution.
3) The simulation results show that the proposed method has an accuracy of 98.5% in predicting the cascading failure probability, and the coincidence degree of identifying key lines exceeds 80%, which provides a scientific basis for power grid planning.
4) The research further puts forward the targeted optimisation strategy. The redundant design of high-risk lines can reduce the probability of large-scale power outage by about 23%, and the rapid response energy storage system can reduce the photovoltaic fluctuation entropy by 35%, which significantly enhances the system flexibility.
5) Limitations and future research directions: This model is currently mainly verified in medium-voltage grid scenarios, and its applicability to ultra-high voltage (UHV) grid scenarios needs further testing. In addition, the model omits the dynamic response characteristics of energy storage devices, and future research can integrate the charging-discharging response mechanism of energy storage into the fault propagation model. For engineering applications, the model can be deployed in actual grid dispatch systems through parallel computing optimisation to improve calculation efficiency, and provide real-time decision support for grid operation and maintenance.

Declaration

All authors declare that they have no conflicts of interest.

References

Altan, G. (2024) 'Analysis of fault ride through the improvement of PV power plant based on capacitive bridge fault current limiter using machine learning', *Electric Power Components and Systems*, Vol. 52, No. 10, pp.1892–1905. https://doi.org/10.1080/15325008.2023.2298704

Almeida, D.R.L., Lima, C.D.N.R. and Junior, M.R.J. (2024) 'Analysis of fault current contributions from small-scale single-phase photovoltaic inverters and their impacts on the protection of electric power distribution systems', *IET Generation, Transmission & Distribution*, Vol. 18, No. 7, pp.1343–1359. https://doi.org/10.1049/GTD2.13127

Bhagwat, A., Dutta, S. and Jadoun, K.V. (2024) 'A customised artificial neural network for power distribution system fault detection', *IET Generation, Transmission & Distribution*, Vol. 18, No. 11, pp.2105–2118. https://doi.org/10.1049/GTD2.13186

Cai, Z., Xiao, W., Sun, H., Luo, C., Zhang, Y., Wan, K., Li, Y., Zhou, Y., Chang, L.-W., Gu, J., Dong, Z., Anandkumar, A., Asi, A. and Hu, J. (2025) 'R-KV: Redundancy-aware KV cache compression for training-free reasoning models acceleration', *arXiv preprint arXiv:2505.24133*. https://arxiv.org/abs/2505.24133

Changjiu, J., Jixu, C., Li, Q., et al. (2023) 'Integrated operation and maintenance of power system communication based on the Markov model', *Applied Mathematics and Nonlinear Sciences*, Vol. 8, No. 2, pp.2453–2462. https://doi.org/10.2478/AMNS.2023.1.00426

Chowdhury, R.B.S., Roy, S., Maji, A., et al. (2024) 'Enhancing LVRT capability of single stage grid connected PV system in accordance with Indian grid code using proportional direct axis current control technique', *Electrical Engineering*, Vol. 107, No. 2, pp.1575–1605. https://doi.org/10.1007/S00202-024-02568-5

Deng, H., Wang, X., Zhong, Y., et al. (2024) 'Grid interlocking fault prevention and control method considering safety and network loss', *Electrical Engineering*, Vol. 106, No. 5, pp.5625–5637. https://doi.org/10.1007/S00202-024-02320-Z

Eshghabad, R.J., Shivaie, M. and Weinsier, D.P. (2024) 'A transfer-learning-based robust technique for multi-type fault detection and classification using Hilbert–Huang transform in low-voltage power distribution grids', *Neural Computing and Applications*, Vol. 36, No. 26, pp.16125–16139. https://doi.org/10.1007/S00521-024-10007-6

Fang, Z., Yang, R., Cai, X., et al. (2023) 'Harmonic suppression and fault ride-through method of diode-rectifier-based hybrid high-voltage direct current system for offshore wind farms integration', *IET Generation, Transmission & Distribution*, Vol. 17, No. 15, pp.3364–3375. https://doi.org/10.1049/GTD2.12835

Kulkarni, N.G. and Virulkar, V.B. (2023) 'Enhancing the power quality of grid connected photovoltaic system during fault ride through: a comprehensive overview', *Journal of The Institution of Engineers (India): Series B*, Vol. 104, No. 3, pp.821–836. https://doi.org/10.1007/S40031-023-00870-7

Javadianpoor, E. and Ajoudanian, S. (2024) 'Formal specification of smart grids for cascading-failures analysis using Alloy modelling language', *International Journal of Grid and Utility Computing*, Vol. 15, No. 6, pp.529–542. https://doi.org/10.1504/IJGUC.2024.142752

Jia, L. (2025) 'Application of anti-voltage sag technology and traveling wave fault location in oilfield power grids', *Journal of Innovation and Development*, Vol. 11, No. 1, pp.64–68. https://doi.org/10.54097/839H0346

Lal, R.M., Avik, B. and Khatod, D.K. (2023) 'Novel control strategy for CESS integrated DC microgrid with on grid and off grid application', *Arabian Journal for Science and Engineering*, Vol. 48, No. 11, pp.14681–14696. https://doi.org/10.1007/S13369-023-07796-8

Li, X., Ma, Y., Ye, K., Cao, J., Zhou, M. and Zhou, Y. (2025) 'Hy-Facial: Hybrid feature extraction by dimensionality reduction methods for enhanced facial expression classification', *arXiv preprint arXiv:2509.26614*. https://arxiv.org/abs/2509.26614

Lijian, Q. and Guohui, Z. (2023) 'DC fault current-limiting method based on dual-loop active control for modular multilevel converters', *COMPEL - The International Journal for Computation and Mathematics in Electrical and Electronic Engineering*, Vol. 42, No. 2, pp.526–542. https://doi.org/10.1108/COMPEL-04-2022-0141

Liu, K., Liu, M., Tang, M., et al. (2025) 'XGBoost-based power grid fault prediction with feature enhancement: application to meteorology', *Computers, Materials & Continua*, Vol. 82, No. 2, pp.2893–2908. https://doi.org/10.32604/CMC.2024.057074

Liu, P., Zhang, Y., Dai, Y., et al. (2024) 'Arc grounding fault identification using integrated characteristics in the power grid', *Energy Engineering*, Vol. 121, No. 7, pp.1883–1901. https://doi.org/10.32604/EE.2024.049318

Noman, M., Ullah, I. and Khan, M.A. (2024) 'Analysis of overcurrent protective relaying as minimum adopted fault protection for small-scale hydropower plants', *International Journal of Environmental Science and Technology*, Vol. 21, No. 4, pp.4457–4470. https://doi.org/10.1007/S13762-023-05284-Y

Meng, L., Xuan, L. and Xueying, H. (2024) 'Intelligent distribution network fault monitoring integrating differential evolution and chaos whale optimization algorithm', *Intelligent Decision Technologies*, Vol. 18, No. 3, pp.1763–1774. https://doi.org/10.3233/IDT-240720

Munna, K. and Jitendra, K. (2023) 'A solution to islanding event detection using superimposed negative sequence components-based scheme', *Arabian Journal for Science and Engineering*, Vol. 48, No. 11, pp.14639–14653. https://doi.org/10.1007/S13369-023-07787-9

Na, X., Bai, P., Xin, L., et al. (2023) 'Research on the construction and implementation of power grid fault handling knowledge graphs', *Energy Reports*, Vol. 9(S2), pp.182–189. https://doi.org/10.1016/J.EGYR.2023.02.073

Nishtar, Z., Wang, F., Jaskani, H.F., et al. (2025) 'Real-time fault detection and isolation in power systems for improved digital grid stability using an intelligent neuro-fuzzy logic', *Computer Modeling in Engineering & Sciences*, Vol. 143, No. 3, pp.2919–2956. https://doi.org/10.32604/CMES.2025.065098

Petrova, Y.S. (2025) 'Fault diagnosis of power grid equipment based on artificial intelligence with limited data', *International Journal of Energy and Water Resources*, Vol. 9, No. 4, pp.1–11. https://doi.org/10.1007/S42108-024-00315-X

Qusay, S., Rafat, A., Khaled, A., et al. (2023) 'An implementation of an enhanced DG primary control equipped with fault detection scheme', *International Journal of Sustainable Energy*, Vol. 42, No. 1, pp.318–330. https://doi.org/10.1080/14786451.2023.2191149

Saad, S., Zakaria, B., Samira, C., et al. (2024) 'Optimizing the power quality of the MV distribution network in fault condition based on D-STATCOM in accordance with the Moroccan Grid Code requirements', *IFAC PapersOnLine*, Vol. 58, No. 13, pp.122–127. https://doi.org/10.1016/J.IFACOL.2024.07.470

Tiefeng, X., Tao, W., Xianwei, J., et al. (2023) 'Power grid fault event reasoning based on entity extraction model of knowledge map', *Journal of Intelligent & Fuzzy Systems*, Vol. 45, No. 5, pp.8479–8488. https://doi.org/10.3233/JIFS-232370

Xueting, C., Ziqi, Z., Yueshuang, B., et al. (2023) 'Identification of high-risk scenarios for cascading failures in new energy power grids based on deep embedding clustering algorithms', *Energy Engineering*, Vol. 120, No. 11, pp.2517–2529. https://doi.org/10.32604/EE.2023.042633

Yahdou, A., Djilali, B.A., Bounadja, E., et al. (2024) 'Using neural network super-twisting sliding mode to improve power control of a dual-rotor wind turbine system in normal and unbalanced grid fault modes', *International Journal of Circuit Theory and Applications*, Vol. 52, No. 9, pp.4323–4347. https://doi.org/10.1002/CTA.3960

Yirun, J., Guo, P. and Qin, L. (2024) 'Converter non-blocking DC fault ride-through and system fast restoration arrangements in R-L SFCL-equipped MMC-M2TDC system', *IET Generation, Transmission & Distribution*, Vol. 18, No. 23, pp.3817–3828. https://doi.org/10.1049/GTD2.13216

Zhang, C., Xu, Y., Chen, Y., et al. (2025) 'Coupling modelling and fault propagation simulation method for power grid-centric urban lifeline systems under extreme disasters', *Energy Internet*, Vol. 2, No. 3, pp.255–273. https://doi.org/10.1049/EIN2.70010

Zhang, H., Guo, J., Li, K., Zhang, Y. and Zhao, Y. (2024) 'Offline signature verification based on feature disentangling aided variational autoencoder', *2024 5th International Conference on Machine Learning and Computer Application (ICMLCA)*, Hangzhou, China, pp.549–554. doi: 10.1109/ICMLCA63499.2024.10754373.

Zhu, Y., Su, R., Wu, J., et al. (2025) 'Multiple fault diagnosis method for regional power grid based on DTS simulation system', *International Journal of Energy Technology and Policy*, Vol. 20, Nos. 1/2, pp.89–94. https://doi.org/10.1504/IJETP.2025.144302